

Supporting Information for

Graphene mediated improved sodium storage in nanocrystalline anatase TiO₂ for sodium ion batteries

Shyamal K Das,^{b*} Birte Jache,^a Homen Lahon,^b Conrad L. Bender,^a Jurgen Janek^{a*} and Philipp Adelhelm,^{c*}

Experimental details

Synthesis of graphene-TiO₂: The graphene-TiO₂ composite were synthesized by a solvothermal method. Titanium tetraisopropoxide (TTIP, Sigma Aldrich) was used as the titania precursor. Graphene (Graphene platelet nanopowder) was commercially available from Sisco Research Laboratories Pvt. Ltd. India. The specified thickness is 6-8 nm, surface area is 150 m²g⁻¹. The graphene nanopowder was treated with concentrated HNO₃ for 24 hr and washed thoroughly by distilled water several times. The acid treated graphene was dispersed in distilled water.

For a typical synthesis of TiO₂-graphene composite, 30 mg of acid treated graphene was dispersed in 26 ml water-ethanol (50% v/v) mixture by ultrasonication for 30 min. Then, 2.6 g of sucrose was dissolved and 2.73 ml concentrated HCl was added. After being stirred for 15 min, 3.9 ml of titanium tetraisopropoxide was added slowly under stirring condition. The solution was stirred for 30 min. The solution was then transferred to a Teflon-lined stainless steel autoclave of capacity 50 ml and heated at 160 °C for 6 h and then cooled to room temperature. The resultant black product was recovered by centrifugation and washed with deionized water and ethanol several times and dried at 110 °C for 24 h. The dried product was calcined at 450 °C for 3 h in air at a heating rate of 2 °C min⁻¹. The pristine TiO₂ was synthesized following the same procedure except adding graphene in the solution. The materials were designated as TiO₂-G and TiO₂ corresponding to the graphene-TiO₂ composite and pristine TiO₂ respectively.

Characterizations: The crystallographic phase identification was performed using powder X-ray diffraction (PANanalytical EMPYREAN; Cu-K_α radiation, λ = 1.5406 Å). The morphology was observed by field emission scanning electron microscopy (Zeiss SMT) and transmission electron microscopy (TEM, FEI Tecnai G2 T12). Specific surface area

(BET) and pore size distribution were obtained from nitrogen adsorption-desorption isotherms (Quantachrome). Thermogravimetric analysis (Shimadzu) was performed under oxygen at a heating rate of 5 °C/min. Elemental analysis was performed with a Vario microcube machine from Elementaranalyse GmbH. Raman spectra (Bruker, 2 mW laser power) were recorded with excitation of 514.5 nm.

Electrode slurries were made from TiO₂-G or TiO₂, polyvinylidene fluoride (PVDF Solef 1013, Solvay), and N-methyl-2-pyrrolidone (NMP, Sigma Aldrich). The weight ratio is TiO₂:Super P Li:PVDF = 80:10:10. Electrodes were prepared by doctor blading a slurry of above composite onto copper foil (Schlenk, d = 10 μm). The thicknesses of the electrodes were approximately around 40–50 μm in the dried state. Circular electrodes (d=1.2 cm) were punched out and contained 3–4 mg active mass each. These were further dried at 120 °C for 2 h under vacuum to evaporate residual NMP and then transferred into an argon-filled glove box (GS Glovebox System Technik). Two electrode coin cells (CR2032, MTI Corporation) were assembled for galvanostatic cycling and cyclic voltammetry. Sodium (BASF) was used as the counter and reference electrodes. Whatman glass microfiber filters (GF/A) were used as separators. The utilized electrolytes were 0.5 M NaPF₆ in diglyme (purity > 99.5 %, Sigma Aldrich) and 0.5 M NaClO₄ in 1:1 w/w EC/DMC (purity>99.0%, Sigma Aldrich). Electrochemical measurements were conducted at 25 °C in a climate cabinet using a Maccor battery cycler (Model 4300). Cells were cycled galvanostatically (constant current) at different current rates between 0.05 V and 2.5 V. Furthermore, cyclic voltammetry was conducted (Biologic VMP3) with different voltage sweep rates in the range of 0.01-2.5 mVs⁻¹ at 25 °C in a climate cabinet.

Supplementary Figures

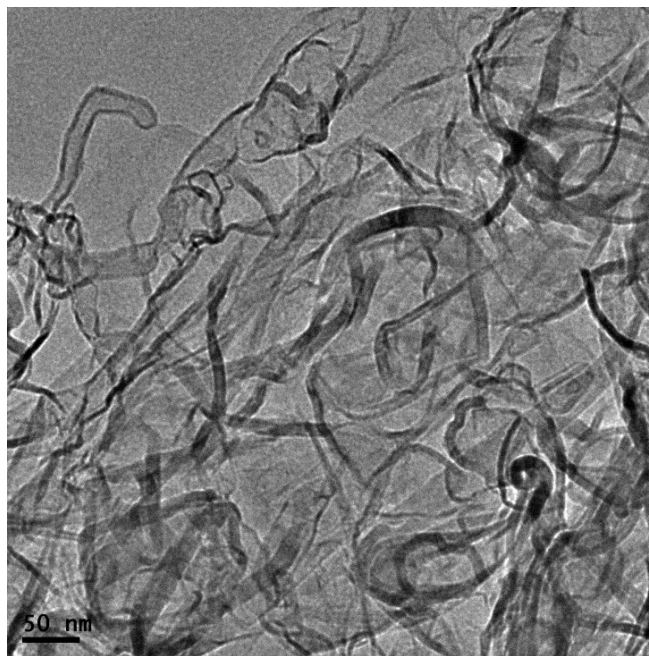


Figure S1. TEM micrograph of pristine graphene.

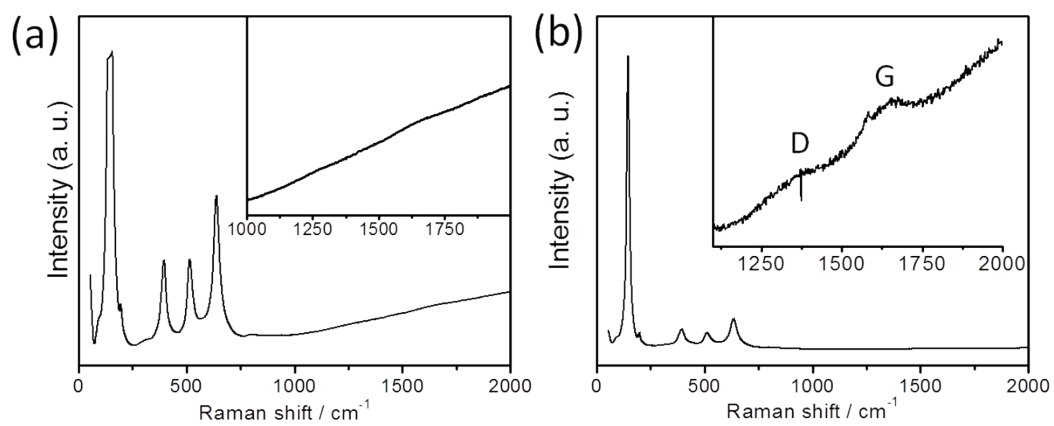


Figure S2. Raman spectra of (a) pristine TiO_2 and (B) TiO_2 -G. Insets show the enlarged view in the range of 1000-2000 cm^{-1} . [Ref S1]

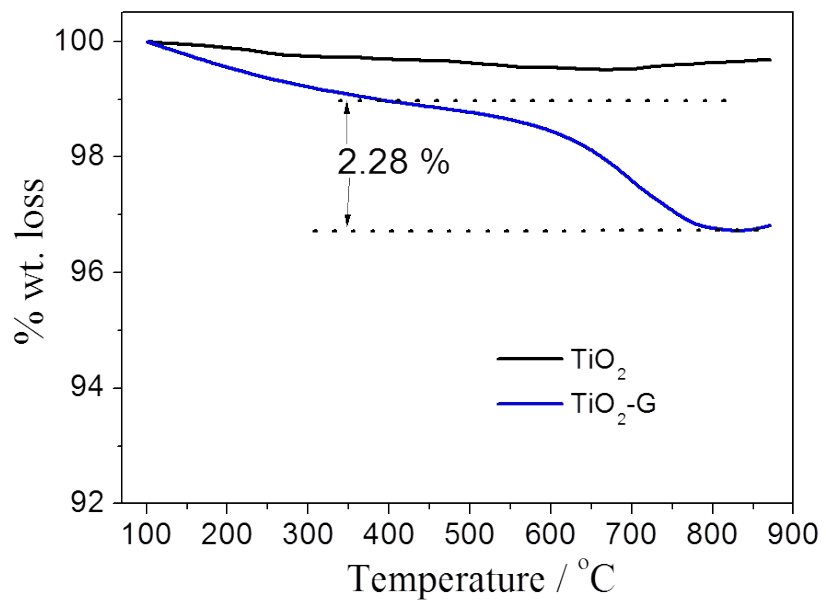


Figure S3. Thermogravimetric analysis of pristine TiO₂ and TiO₂-G.

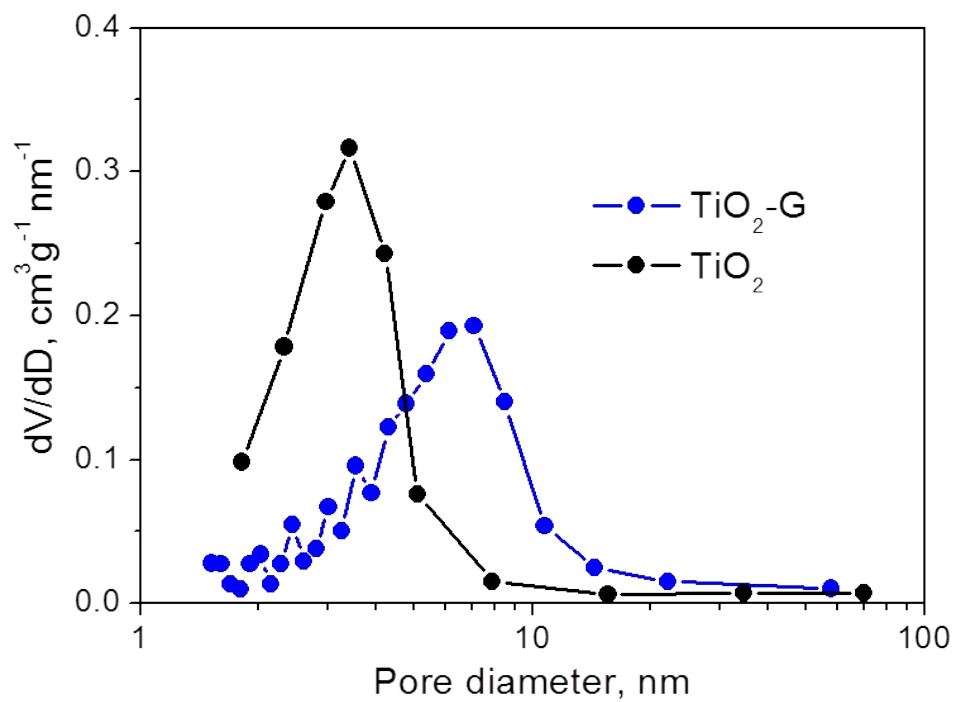


Figure S4. BJH pore size distributions (obtained from adsorption isotherm) of pristine TiO₂ and TiO₂-G.

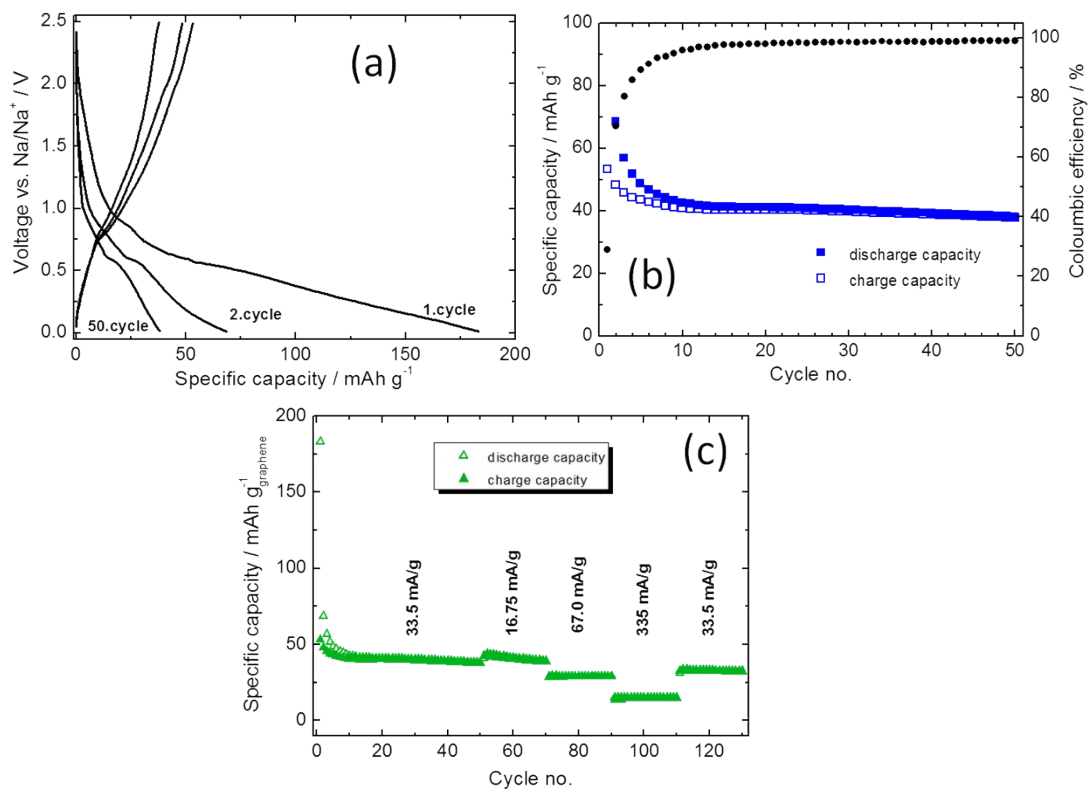


Figure S5. (a) Galvanostatic charge/discharge curves of pristine graphene at a current density of 33.5 mA/g at 25 °C, (b) variation of capacities and coulombic efficiencies with cycle number at 33.5 mA/g and (c) variation of capacities with cycle number at different current rates. The used electrolyte solvent is diglyme.

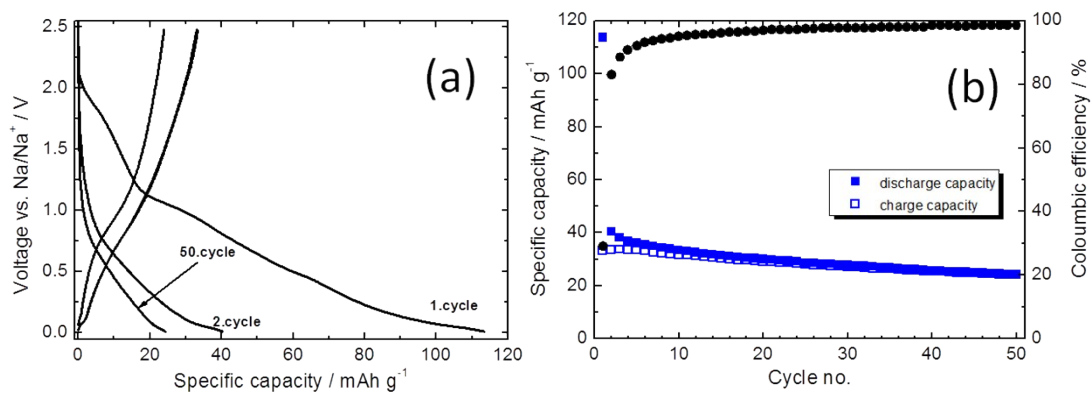


Figure S6. (a) Galvanostatic charge/discharge curves of pristine TiO_2 at a current density of 33.5 mA g^{-1} at $25 \text{ }^\circ\text{C}$ and (b) variation of capacities and coulombic efficiency with cycle number at 33.5 mA g^{-1} . The used electrolyte solvent is EC/DMC.

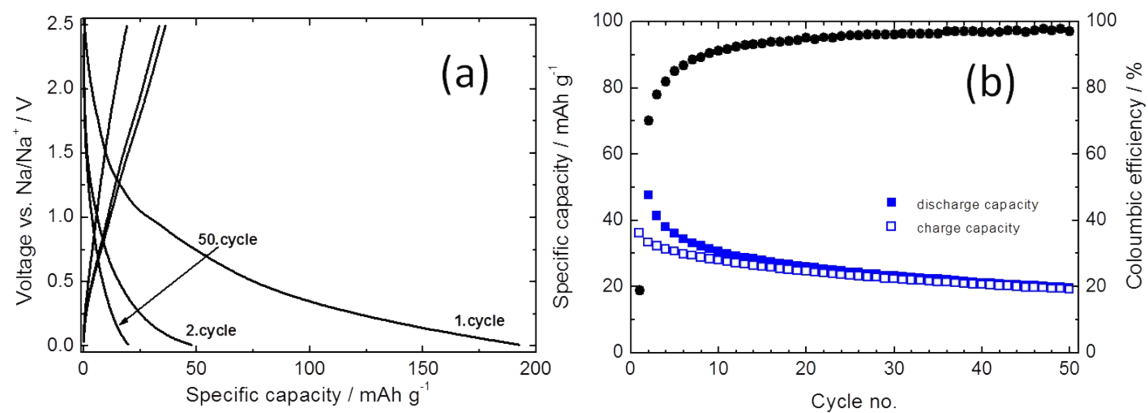


Figure S7. (a) Galvanostatic charge/discharge curves of pristine graphene at a current density of 33.5 mA g⁻¹ at 25 °C and (b) variation of capacities and coulombic efficiency with cycle number at 33.5 mA g⁻¹. The used electrolyte solvent is EC/DMC.

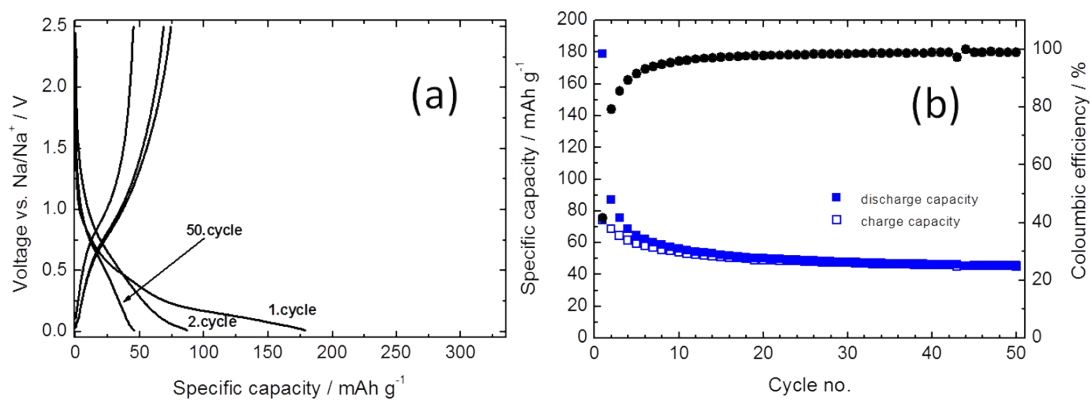


Figure S8. (a) Galvanostatic charge/discharge curves of TiO₂-G at a current density of 33.5 mA g⁻¹ at 25 °C and (b) variation of capacities and coulombic efficiencies with cycle number at 33.5 mA g⁻¹. The used electrolyte solvent is EC/DMC.

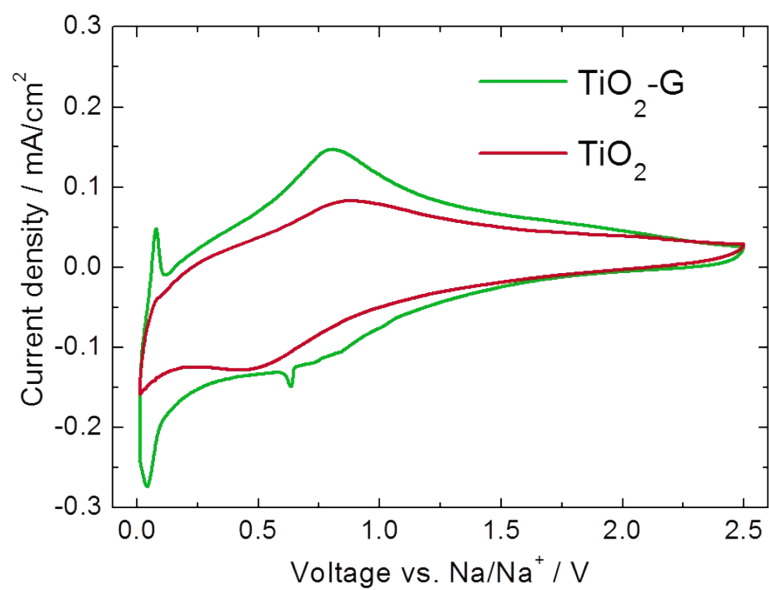


Figure S9. 3rd cycle cyclic voltammetry curves of TiO₂-G and TiO₂ for comparison. The scan rate is 0.05 mV/s. The used electrolyte solvent is diglyme.

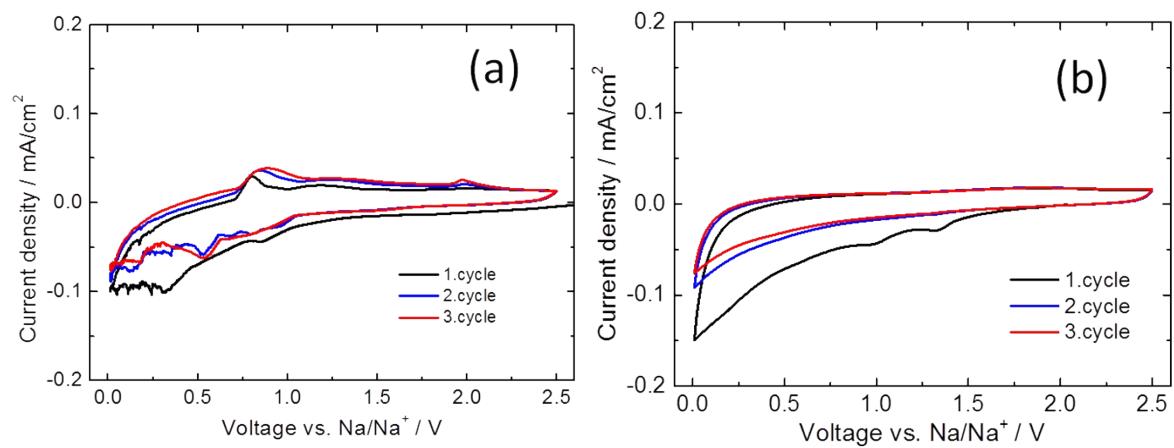


Figure S10. Cyclic voltammety curves of pristine graphene at a scan rate is 0.05 mV/s at 25 °C in (a) diglyme and (b) carbonate electrolytes.

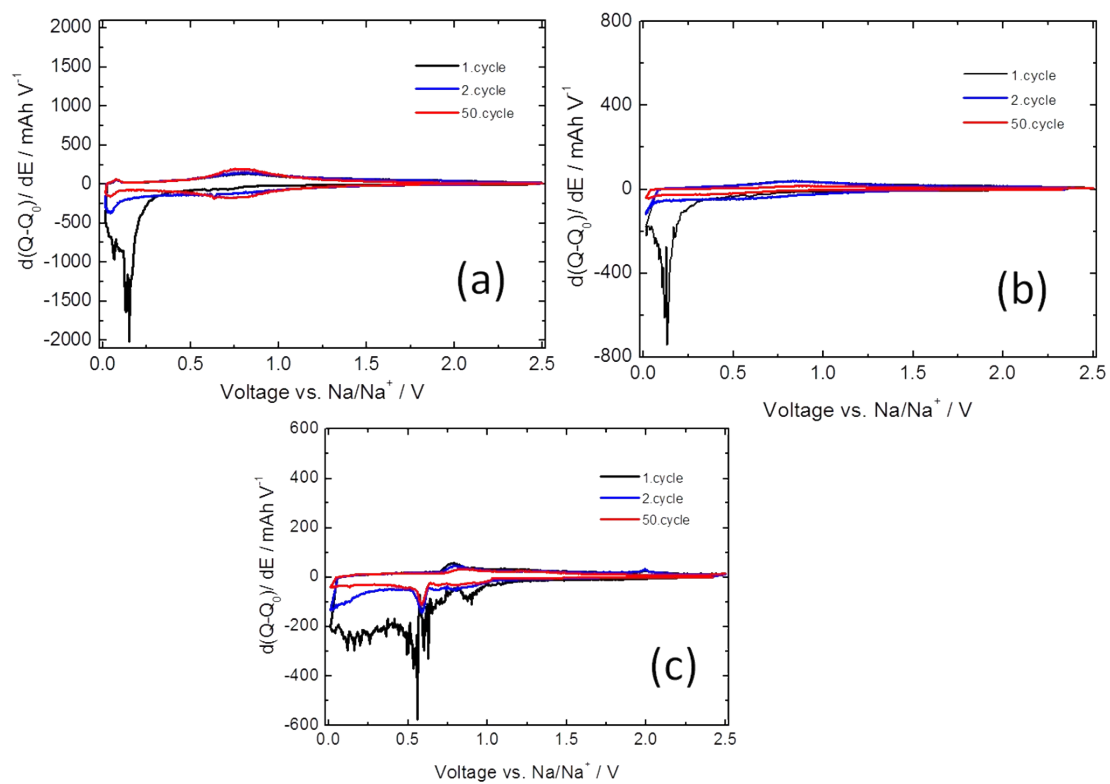


Figure S11. Differential capacity plots for (a) TiO₂-G, (b) TiO₂ and (c) graphene cycled at 33.5 mA g⁻¹ at 25 °C in diglyme electrolyte.

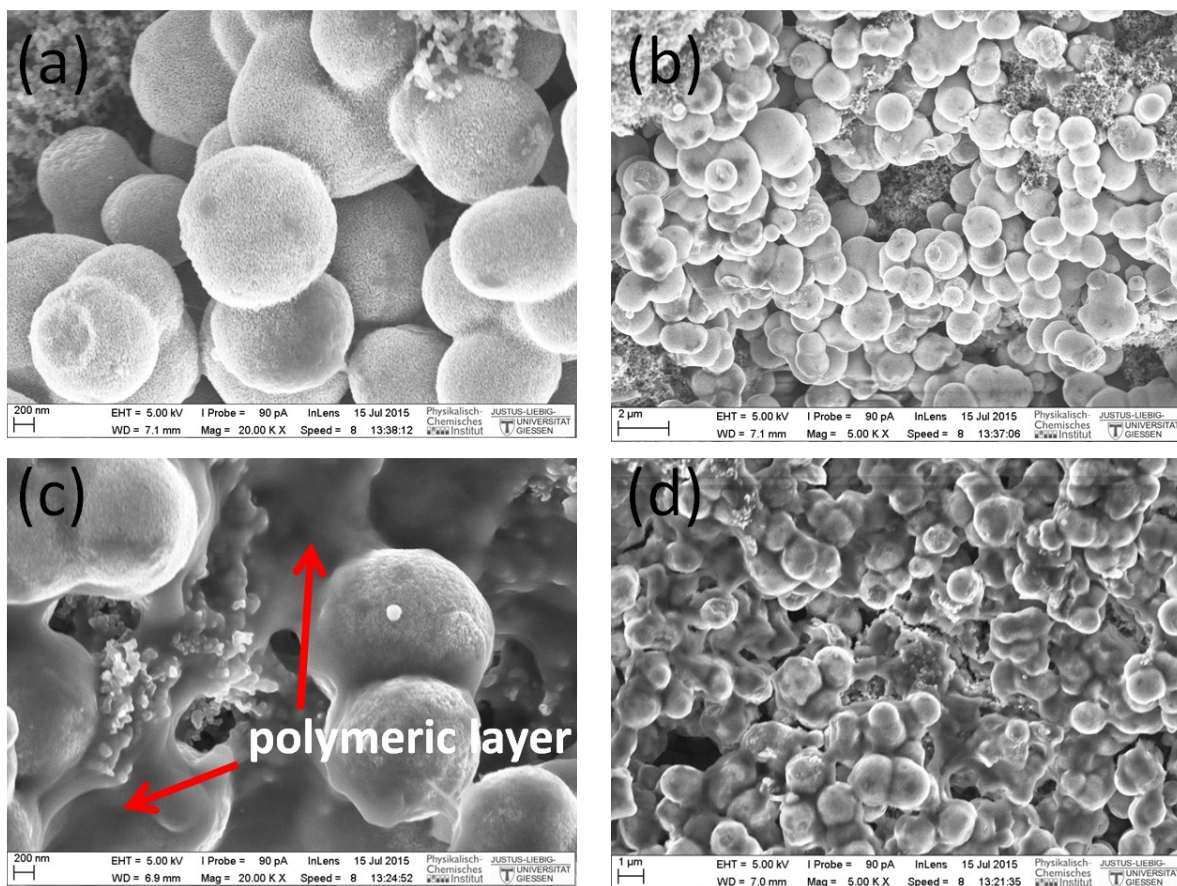


Figure S12. Ex-situ SEM micrographs of discharged product of $\text{TiO}_2\text{-G}$ in (a, b) diglyme and (c, d) carbonate electrolytes.

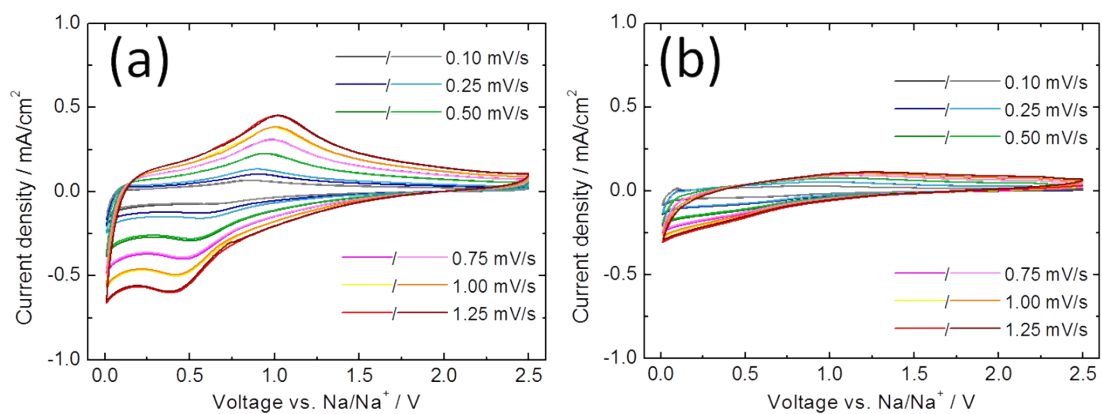


Figure S13. Cyclic voltammetry curves of (a) TiO₂-G and (b) TiO₂ at different scan rates in carbonate electrolytes.

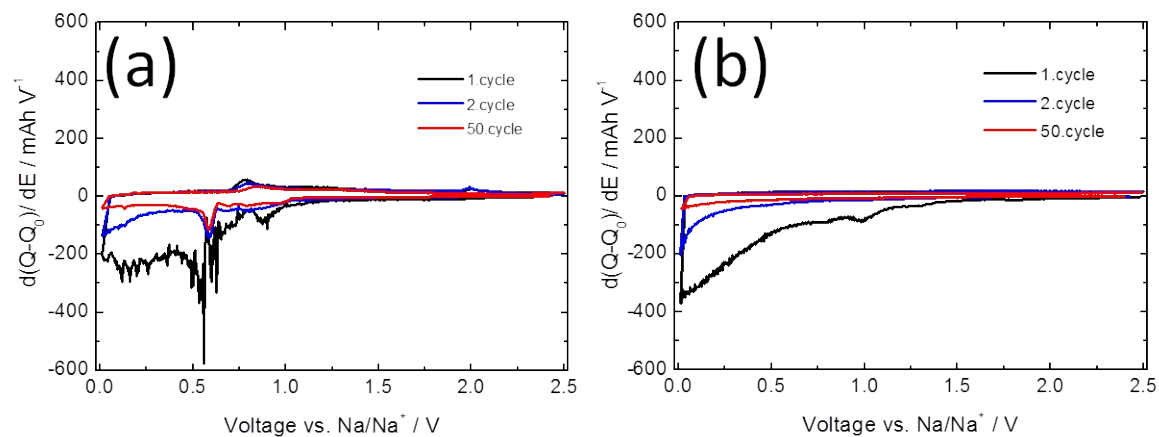


Figure S14. Differential capacity plots for pristine graphene cycled at 33.5 mA g^{-1} at 25°C in (a) diglyme and (b) carbonate electrolyte.

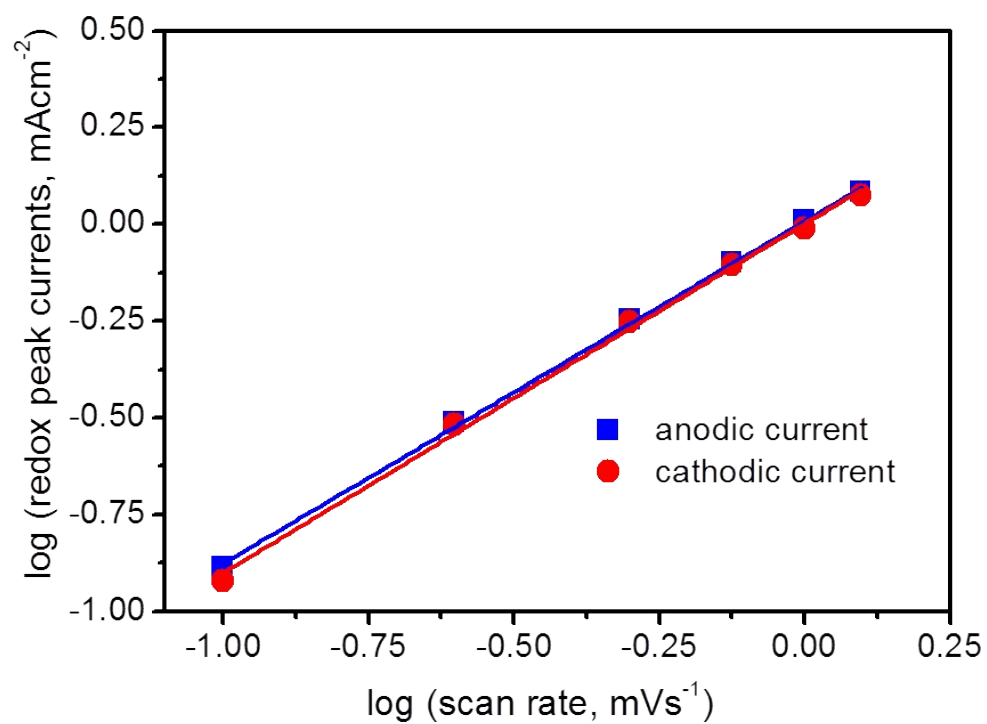


Figure S15. Determination of the b-value using the relationship $I = a\gamma^b$ for TiO₂-G using the CV data of figure 3c (main text).

Supplementary Table

Table S1: Comparison of initial Coulombic efficiencies of few reported TiO₂.

Material	Electrolyte solvent	Current density (mA _g ⁻¹)	Initial Coulombic efficiency %	Reference
TiO₂-graphene	Diglyme	35.6	60	This work
TiO ₂ @rGO	PC+FEC	100	~ 35	[1]
TiO ₂	PC	36.9	~ 40	[2]
	EC+PC		~ 45	
	EC+DMC		~ 17	
TiO ₂ -graphene	EC+PC	50	~ 27	[3]
TiO ₂	PC	33.6	~ 38	[4]
TiO ₂ -carbon	PC+FEC	10	< 30	[5]
TiO ₂ -carbon	PC+FEC	0.5C	50.6	[6]
TiO ₂	EC+DEC	50	55	[7]
TiO ₂ -carbon	EC+DMC	30	57	[8]
TiO ₂ - carbon	PC+FEC	20	~ 37	[9]
Ni-TiO ₂	PC	50	~ 30	[10]
TiO ₂	EC+DEC	85	46.1	[11]
TiO ₂ -carbon	EC+PC	16.8	< 40	[12]
TiO ₂ -carbon	EC+DEC	50	41.9	[13]
Sn- TiO ₂	EC+PC	50	~ 35	[14]
TiO ₂ -carbon	EC+PC	100	25.7	[15]

(PC: propylene carbonate, FEC: fluoroethylene carbonate, DMC: dimethyl carbonate, EC: ethylene carbonate, DEC: diethyl carbonate)

References:

- S1. H. Liu, K. Cao, X. Xu, L. Jiao, Y. Wang, and H. Yuan, *ACS Appl. Mater. Interfaces*, 2015, **7**, 11239
- S2. L. Wu, D. Buchholz, D. Bresser, L. G. Chagas and S. Passerini, *J. Power Sources*, 2014, **251**, 379
- S3. C. Chen, Y. Wen, X. Hu, X. Ji, M. Yan, L. Mai, P. Hu, B. Shan, Y. Huang, *Nature Commun.*, 2015, DOI: 10.1038/ncomms7929
- S4. X. Yang, C. Wang, Y. Yang, Y. Zhang, X. Jia, J. Chen and X. Ji, *J. Mater. Chem. A*, 2015, **3**, 8800
- S5. K. Kim, G. Ali, K. Y. Chung, C. S. Yoon, H. Yashiro, Y. K. Sun, J. Lu, K. Amine and S. T. Myung, *Nano Lett.*, 2014, **14**, 416
- S6. Y. Zhang, Y. Yang, H. Hou, X. Yang, J. Chen, M. Jing, X. Jia and X. Ji, *J. Mater. Chem. A*, 2015, **3**, 18944
- S7. Z. Hong, K. Zhou, J. Zhang, Z. Huang and M. Wei, *J. Mater. Chem. A*, 2015, **3**, 17412
- S8. Y. Ge, H. Jiang, J. Zhu, Y. Lu, C. Chen, Y. Hu, Y. Qiu, X. Zhang, *Electrochimica Acta*, 2015, **157**, 142

- S9. S. M. Oh, J. Y. Hwang, C. S. Yoon, J. Lu, K. Amine, I. Belharouak, and Y. K. Sun, *ACS Appl. Mater. Interfaces*, 2014, **6**, 11295
- S10. Y. Xu, M. Zhou, L. Wen, C. Wang, H. Zhao, Y. Mi, L. Liang, Q. Fu, M. Wu, and Y. Lei, *Chem. Mater.*, 2015, **27**, 4274
- S11. Z. Hong, K. Zhou, Z. Huang and M. Wei, *Scientific Reports*, 2015, Doi: 10.1038/srep11960
- S12. D. Bresser, B. Oschmann, M. N. Tahir, F. Mueller, I. Lieberwirth, W. Tremel, R. Zentel and S. Passerini, *J. Electrochem. Soc.*, 2015, **162**, A3013
- S13. Y. Xu, E. M. Lotfabad, H. Wang, B. Farbod, Z. Xu, A. Kohandehghan and D. Mitlin, *Chem. Commun.*, 2013, **49**, 8973
- S14. D. Yan, C. Yu, Y. Bai, W. Zhang, T. Chen, B. Hu, Z. Sun and L. Pan, *Chem. Commun.*, 2015, **51**, 8261
- S15. F. Yang, Z. Zhang, Y. Han, K. Du, Y. Lai and J. Li, *Electrochimica Acta*, 2015, **178**, 871